



Generation of PM₁₀ Map with Sentinel-2 Satellite Images: The Case of Çankırı Province

*Makale Bilgisi / Article Info

Alındı/Received: 07.10.2023

Kabul/Accepted: 09.03.2024

Yayımlandı/Published: 29.04.2024

Sentinel-2 Uydu Görüntüleri ile PM₁₀ Haritasının Üretilmesi: Çankırı İli Örneği

Osman KARAKOÇ^{1*}, Semih EKERCİN²

¹Necmettin Erbakan Üniversitesi, Mühendislik Fakültesi, Harita Mühendisliği Bölümü, Konya, Türkiye

²Antalya Bilim Üniversitesi, Antalya, Türkiye

© Afyon Kocatepe Üniversitesi

Abstract

Air pollution, which is characterized as a global environmental problem, negatively affects life in Turkey as a result of the increase in the amount of energy needed and uncontrolled construction. In order to minimize the health impacts of air pollution, air quality should be monitored regularly and necessary steps should be taken to improve it. With the innovations in satellite technologies, the air quality of large areas can be monitored with the help of satellite images and effective solutions can be produced in many areas such as the detection of air pollutant parameters and the creation of thematic maps. The main objective of the research is to investigate the relationship between in-situ measured PM₁₀ parameters and Sentinel-2 satellite data and to map PM₁₀ based on this relationship. In this context, PM₁₀ parameters measured in the field on two different dates and Sentinel-2 satellite images dated 22.11.2021 and 16.04.2022 were used as data sources. The relationship between the data used was established by multiple regression analysis. The coefficients obtained from the analysis results were applied to the relevant bands and thematic maps were created using satellite images. The correlation coefficients of 0.80 and 0.79 calculated by regression analyses indicate that sufficient accuracy was achieved in the research. The results of the study show that satellite imagery provides accurate data for PM₁₀ estimate and that pollution exceeds World Health Organization limits in the road transportation network and industrial areas.

Keywords

Remote sensing; Air pollution; Regression analysis; PM₁₀; Sentinel-2

Öz

Küresel boyutta çevresel bir problem olarak nitelendirilen hava kirliliği dünya ülkelerine benzer şekilde Türkiye’de de gereksinim duyulan enerji miktarındaki artışın ve kontrolsüz yapılaşmanın bir sonucu olarak yaşamı negatif yönde etkilemektedir. Hava kirliliğine bağlı sağlık etkilerinin minimum düzeye indirilmesi için hava kalitesinin düzenli periyotlarla izlenmesi ve iyileştirilmesi yönünde ihtiyaç duyulan adımların atılması gerekmektedir. Uydu teknolojilerindeki yenilikler ile birlikte büyük alanların hava kalitesi uydu görüntüleri yardımıyla izlenebilmekte ve hava kirlileti parametrelerin saptanması, tematik haritaların oluşturulması gibi birçok alanda etkili çözümler üretilebilmektedir. Araştırmanın temel amacı yerinde ölçülen PM₁₀ parametreleri ile Sentinel-2 uydu verileri arasındaki ilişkiyi araştırmak ve bu ilişkiye dayanarak PM₁₀’u haritalandırmaktır. Bu kapsamda çalışmada farklı iki tarihte arazide ölçülen PM₁₀ parametreleri ile Sentinel-2 uydusuna ait 22.11.2021 ve 16.04.2022 tarihli görüntüler veri kaynakları olarak kullanılmıştır. Kullanılan veriler arasındaki ilişki çoklu regresyon analizi ile kurulmuştur. Analiz sonuçlarından temin edilen katsayılar ilgili bantlara uygulanmış ve uydu görüntüleri kullanılarak tematik haritalar oluşturulmuştur. Regresyon analizleri ile hesaplanan 0,80 ve 0,79 korelasyon katsayıları araştırmada yeterli doğruluğa ulaşıldığını işaret etmektedir. Çalışma sonuçları PM₁₀ tahmininde uydu görüntülerinin doğru veriler sunduğunu ve kirliliğin karayolu ulaşım ağı ile endüstriyel bölgelerde Dünya Sağlık Örgütü limitlerini aştığını göstermektedir.

Anahtar Kelimeler

Uzaktan algılama; Hava kirliliği; Regresyon analizi; PM₁₀; Sentinel-2

1. Introduction

The world population is expected to reach 9.7 billion in 2050 and 10.4 billion in the 2080s, and to remain at this level until 2100 (UN 2022). Increasing energy demand and uncontrolled urbanization in parallel with rapid population growth negatively affect air quality. According to the World Health Organization's air quality database, 99% of the world's population is behind the WHO air quality limits and is exposed to air pollution at a scale that threatens human health (WHO 2022).

Particulate matter (PM), which causes air pollution, is one of the most dangerous air pollutants because it easily enters the respiratory tract (Kim 2015). Particulate matter, which is part of air pollution, is tiny particles consisting of organic chemicals, metals, acids and dust particles (Jonathan et al. 2012). Particles between 2.5 µm and 10 µm in size are called coarse particles (PM₁₀), those between 0.1 µm and 2.5 µm are called fine particles (PM_{2.5}) and particles smaller than 0.1 µm are called ultrafine particles (UFP) (Tasic et al. 2006). The results of

worldwide epidemiological research revealed the relationship between the number of particles in the environment and the death rates in the population (Schwarze et al. 2006). Developing air pollution with PM causes a variety of cardiovascular and respiratory diseases (Hime et al. 2018). It is estimated that 3% of all developing deaths due to heart and respiratory disease in the world and 5% of developing deaths due to lung cancer have been caused by particle substances (Cohen et al. 2005). It is known that a 10 µg/m³ increase in PM₁₀ level causes an increase in daily mortality rates between 0.5% and 1.5% (Valavanidis et al. 2008). This situation reveals the necessity of studies to be carried out for regular monitoring and control of the PM₁₀ parameter. Due to all these reasons, the PM₁₀ parameter, one of the most important components of air pollution, was used in the study.

Developing air pollution from both natural and artificial sources of PM threatens human health, as well as adversely affects climate conditions. To reduce these adverse effects and contain air pollution, local legislation studies in all countries and the WHO daily (45 µg/m³) and annual (15 µg/m³) limit values and PM₁₀ limits have been established. In Turkey, the "Air Quality Assessment and Management Regulation" and the daily and annual PM₁₀ limit values are set at 50 µg/m³ and 40 µg/m³ respectively. To ensure control of PM₁₀ boundary values, proper monitoring of the number of pollutants and steps towards improving air quality must be taken.

Today, PM₁₀ values can be measured through fixed stations or portable samplers. However, the high installation costs of fixed monitoring stations and the level of data that cannot homogeneously represent a region's air quality, and the low cost of data sensitivity of portable samplers have led to new solutions for the estimation of polluting parameters. Innovations in satellite systems, which are the result of technological developments, provide highly accurate results in estimating major pollution sources using satellite images, monitoring air quality in regions with large surface areas, creating dispersion models for air quality and producing thematic maps. In fact, there are several studies in international literature aimed at estimating satellite images and air pollutant parameters (Karakoç 2022).

Harbula (2010), tested the relationship between Aerosol Optical Depth (AOD) data from the Modis sensor and PM₁₀ parameters. The regression analysis has determined that PM₁₀ values are in a meaningful relationship with the AOD. Wang et al. (2021) developed a new approach for the estimation of daily full-scope ambient concentrations

of PM_{2.5} and PM₁₀ in China using Sentinel-5P TROPOMI and GEOS-FP datasets. Light Gradient Boosting Machine (LGBM) machine learning method was used to estimate the parameters. The correlation coefficients of 0.88 and 0.83 for PM_{2.5} and PM₁₀, respectively, showed that the parameters were successfully estimated by the applied method and thus the model performance was good. Nguyen and Tran (2014), In a study conducted in Hanoi, Vietnam, Landsat-8 implemented regression analysis to determine the relationship between the reflectance values derived from the bands of the satellite image and PM₁₀ data. The correlation coefficient (R=0.888) obtained by regression analysis indicates that the Landsat-8 satellite image and PM₁₀ parameters may be calculated. Makineci et al. (2023) used Sentinel-5P satellite data to examine the status of pollutant parameters in Konya between 2019 and 2021. In the study, the amounts of ozone, methane, carbon monoxide and nitrogen dioxide gases were plotted on a monthly basis and mapped on an annual basis using Sentinel-5P Level-2 data obtained from the Google Earth Engine platform. It was concluded that methane gas is observed in forested areas and large wetlands and reaches its minimum levels in winter, while other gases reach their minimum levels in summer. Jafarian and Behzadi (2020), Using PM_{2.5} data from 23 air quality monitoring stations located in Tehran, Iran, and Landsat-8 satellite imagery, it was tested the relationship between air pollution and satellite images. The relationship between the band values of Landsat satellite images and PM_{2.5} values has been studied by the 19 regression model. The study found that it was possible to estimate PM_{2.5} values by satellite images. Othman et al. (2010) developed a multispectral algorithm in the Mecca, Myna and Arafat regions of Saudi Arabia to predict the concentrations of particulate matter (PM₁₀) using Landsat-7 satellite images. In the application field, coordinates from the PM₁₀ measurement points are taken using GPS. The correlation coefficient (R > 0.8) obtained by regression analysis indicates that this method is reliable. Ghasempour et al. (2021) used nitrogen dioxide (NO₂) and sulfur dioxide (SO₂) data derived from Sentinel-5P and AOD (Aerosol Optical Depth) data derived from MODIS to investigate the impact of Covid-19 pandemic quarantines on air quality in Turkey. The results of the study showed that SO₂ did not change during the quarantine and even increased slightly in some areas, while NO₂ and AOD decreased significantly. When the data obtained were compared with the station data in Istanbul, it was found that there was no significant correlation for SO₂. Correlation coefficients of 0.83, 0.70 and 0.65 for NO₂ and 0.86 and 0.82 for AOD data,

respectively. Sifakis and Deschamps (1992), in their work, estimated the concentration of particulate matter using the SPOT XS1 band in Toulouse, France. The study results show that particulate matter estimation over large areas can be easily done by satellite imaging. Chen et al. (2021) used the Bira-Lambert law and multivariate regression analysis to accurately estimate PM_{2.5} and PM₁₀ values using hyperspectral imaging. It has been found that PM_{2.5} and PM₁₀ can be analyzed in visible, near-infrared and remote infrared light bands and that the accuracy in the visible light band is higher than in other bands. Mamić et al. (2023) estimated PM_{2.5} and PM₁₀ concentrations in their study in Croatia using remote sensing data sets in the Google Earth Engine system with Sentinel-5P. They used a random forest machine learning algorithm to perform spatial modeling of particulate matter spatial distribution. The data obtained from the air quality monitoring station were matched with remote sensing data and seasonal models were trained by machine learning method. The results of the study showed that the method applied in the estimation of PM_{2.5} and PM₁₀ parameters was successful. Li et al. (2019) compared AOD data from Sentinel-2A and Landsat-8 satellite images to local source AOD data. The results of the study determined by the determining coefficient ($R^2 > 0.90$) indicate that the relationship for AOD data is available in urban environments. The Sentinel-2A satellite data was also found to yield higher accuracy compared to Landsat-8.

Although there have been many international studies on the estimation of air pollution with satellite imagery, this issue is not yet common in Turkey. For this reason, this study aims to estimate and thematically map the PM₁₀ parameters causing air pollution Çankırı city center using Sentinel-2 satellite images. In this context, the applicability of the method was investigated in Çankırı city center, which is dense in terms of traffic and population and contains industrial zones.

2. Materials and Methods

2.1 Study area

In this study, the city center of the city of Çankırı was selected as the main application area for the 32° 30' to 34° 10' eastern meridians and the 40° 30' to 41° 33' north parallels (Figure 1).

2.2 Satellite data

Obtaining the images closest to the dates of the fieldwork carried out within the scope of the study is very important

for achieving high accuracy. In addition, another factor affecting the accuracy of the study is that the satellite images to be used should be cloud-free. Sentinel-2 is one of the most advanced satellites offering free data for remote sensing applications. Sentinel-2 satellite provides the opportunity to take images from the same place at 5-day intervals, with its images covering wide areas with high spatial resolution. For these reasons, Sentinel-2 satellite imagery was used in the study, which has a short revisit time and therefore allows cloud-free images to be obtained closest to the field work. The Sentinel-2 satellite has a spatial resolution of 13 spectral bands ranging from 10 m to 60 m and a strip width of 290 km. In this study, a combination of red, green and blue bands with a resolution of 10 m was used because it provides high accuracy in regression analysis. Sentinel-2 satellite imagery from April and November was used to estimate air pollution in more meaningful ways. Satellite images from the spring (16.04.2022) and autumn (22.11.2021) are important for assessing the impact of fossil fuel use and seasonal conditions on PM₁₀ values.

2.3. In-situ data

The implementation part of the study was followed by two field works on 20.11.2021 and 13.04.2022. Particulate samples are to be collected before the field work, and on the relevant dates are localized measurement methods and PM₁₀ measurements from locations within the application area. In both field works, measurements were made at frequent intervals in areas with high fossil fuel use, traffic and population density. In this context, the first field work took measurements from 30 locations and the second field work from 40 locations.

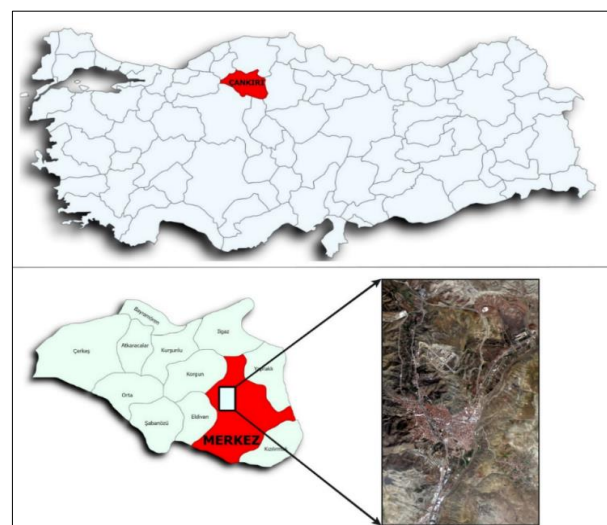


Figure 1. Study area map

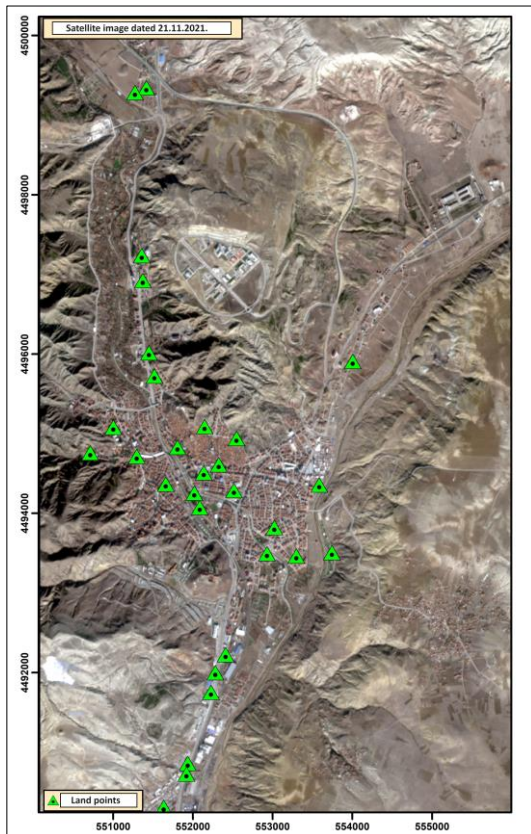


Figure 2. PM₁₀ sampled point locations on 21.11.2021

In this work, the CEM DT-9880 portable air quality measuring device was used to collect PM₁₀ samples. Sampling was performed at all points when the height of the device averaged 1 meter. The measurements worked with a minimum of 2 minutes between each measurement and a measurement time of 1 minute. Also, the locations of the points being measured are taken with the help of handheld GPS.

2.4 Radiometric and atmospheric correction

Radiometric correction is intended to reduce the atmospheric effects that develop during satellite imaging. This is done by converting the pixel brightness values of the image into a unit comparable to the spectral projection values, which are implemented in two phases (Mather et al. 2011). The European Space Agency (ESA) has been providing derived Level-1C products for Sentinel-2A since 2015 and Sentinel-2B since 2017. Level-1C data correspond to reflectance values after radiometric and geometric corrections have been applied. In addition, Copernicus Open Access Center has been providing Level-2A products since March 2017 (Sola et al. 2018). Sentinel-2 satellite images used in the study were obtained as a free registration through the USGS (United States Geological Survey) Earthexplorer system. The downloaded file contains the image file, metadata,

geometric and radiometric correction information for all bands. Atmospheric correction was performed through the SCP (Semi-Automatic Classification Plugin) module integrated into the QGIS software, using the metadata in the downloaded file.

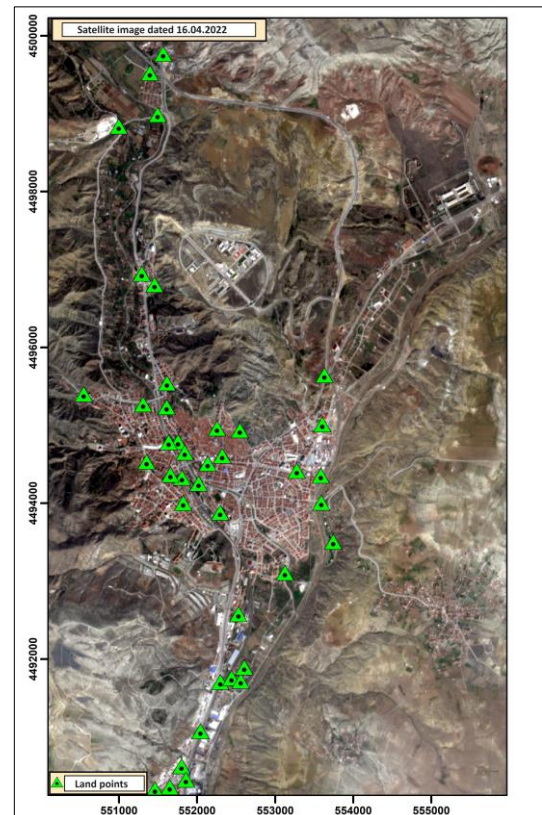


Figure 3. PM₁₀ sampled point locations on 13.04.2022



Figure 4. PM₁₀ measurement device

2.5 Kriging method

Kriging is a method of cutting the optimal values of data from other points by using data from known points. With this method, the parameters to be interpolated in an area are used as a regional variable. The regional variable constantly varies in location so that points close to each

other have a high correlation (İnal et al. 2002). In general, today there are a number of different kriging methods is being used. These methods are ordinary, universal, block, disjunctive and co-kriging (Nas et al. 2007). Ordinary kriging method is mainly used for environmental as a reliable interpolation method in many disciplines, including studies is used. For this reason, ordinary kriging, a geostatistical interpolation method, was used to obtain the spatial distribution of PM₁₀ parameters measured during field studies.

2.6 Regression analysis

Regression analysis is a technique of analysis to determine the relationship between two or more variables with cause-and-effect relationships. The mathematical engine of this technique is the equation of regression (Şahinler 2000). The main objectives of regression analysis, which is one of the most important methods in terms of determining the statistical relationship, are listed as follows;

- To analyze whether one or more independent variables have a significant effect on the dependent variable,
- Estimating the values that the dependent variable can take,
- To examine the effect on the dependent variable specific to the change in the independent variables (Maddala 2001).

The correlation coefficient (*r*) is used in determining the degree to which the regression equation explains the observation value or the degree of the relationship between variables. The correlation coefficient is taking values in the range +1 to -1, giving an idea of the direction of the correlation. Correlation coefficient value;

- *r*=1 state; It means that the relationship between the variables is complete.
- *r*=0 state; which means that there is no relationship between the variables.

Regression analysis method is frequently used for the relationship between satellite images used in remote sensing applications and the studied parameters. In this study, the relationship between in-situ measured PM₁₀ data and satellite image reflectance values was tested by regression analysis. A regression equation was created to estimate PM₁₀ values from satellite images. With the help of this equation, the relationship between PM₁₀ parameters and satellite images was tested. The independent variables of this equation are the reflectance values of the bands (red, green and blue) of the Sentinel-

2 satellite. The dependent variable is PM₁₀ values obtained from field works on two different dates. This triple band combination was used in the regression analysis because it provides higher accuracy. The regression equation is shown below.

$$Y = B_0 + B_1X_{i1} + B_2X_{i2} + \dots + B_pX_{ip} + E_i \quad (1)$$

Y: PM₁₀ values obtained from field works

X_i: Reflectance values obtained from the red, green and blue bands of the Sentinel-2 satellite

i: the band numbers from the satellite image

B: Regression coefficients.

3. Results and Discussion

3.1 Interpolation of data with kriging method

Thematic maps were produced by kriging interpolation using PM₁₀ data measured during both field studies (Figure 5 and Figure 6). Thematic maps obtained by kriging method are important data sources to test the distribution of pollutants in the application area and to show the positive impact of satellite imagery on the accuracy of the study. In both thematics produced by the kriging interpolation method, It has been determined that the areas with high PM₁₀ levels are similar in the map. This shows that the thematic maps produced by the kriging method are consistent.

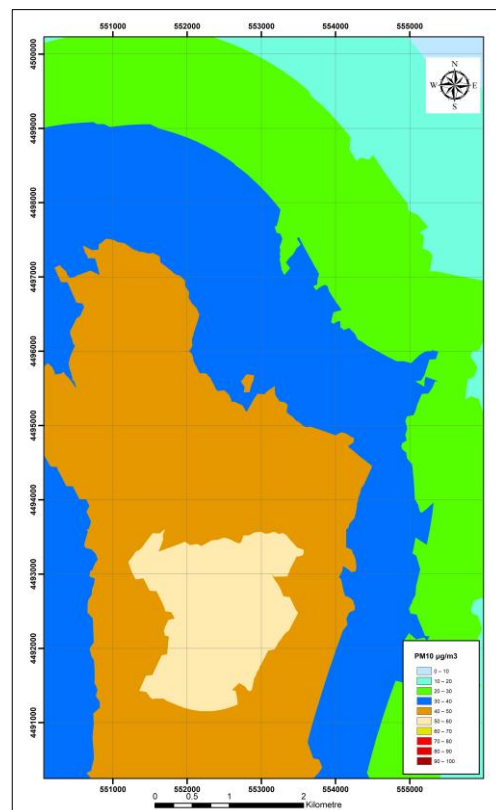


Figure 5. Thematic map dated 20.11.2021 produced with the Kriging method

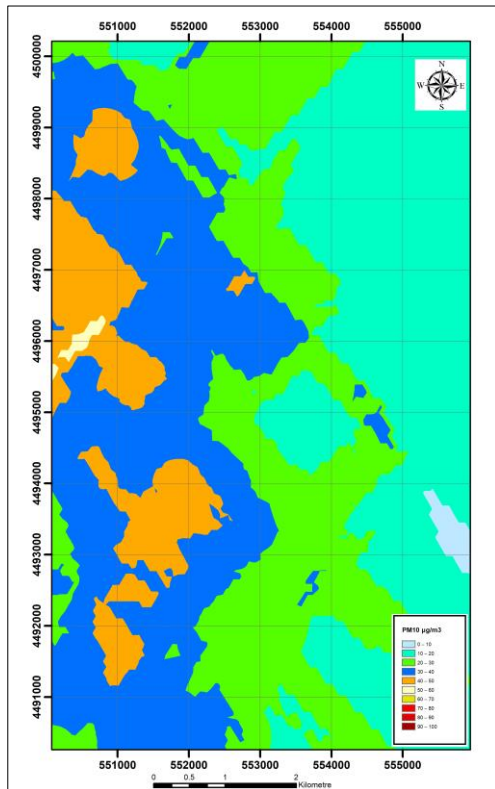


Figure 6. Thematic map dated 13.04.2022 produced with the Kriging method

3.2 Evaluation of the regression model

In the field work dated 20.11.2021, PM₁₀ measurements were made from 30 locations. The PM₁₀ measurement was measured by the hand-held GPS coordinate of each point. All the measured PM₁₀ samples are included in the regression analysis. Regression analysis showed an 80% relationship between the PM₁₀ values obtained from the field work and the model generated (Figure 7). This ratio indicates a high degree of correlation between the PM₁₀ and the Red, Green and Blue bands. The remaining 20% were scattered by other unknown factors. In addition, the Durbin-Watson test statistics, expected to be around 2, were calculated at 2,294. This can be explained by the fact that there are no other factors that affect the dependent variable other than the arguments. Finally, the Sigma value in the Anova table is less than 0.05, indicating the significance of the generated model.

In the field work dated 13.04.2022, PM₁₀ measurements were made from 40 locations. The PM₁₀ measurement was measured by the hand-held GPS coordinate of each point. All the measured PM₁₀ samples are included in the regression analysis. Regression analysis showed a 79% relationship between the PM₁₀ values obtained from the field work and the model generated (Figure 8). This ratio indicates a high degree of correlation between the PM₁₀ and the Red, Green and Blue bands. The remaining 21%

were scattered by other unknown factors. In addition, the Durbin-Watson test statistics, expected to be around 2, were calculated at 1,284. This can be explained by the fact that there are no other factors that affect the dependent variable other than the arguments. Finally, the Sigma value in the Anova table is less than 0.05, indicating the significance of the generated model.

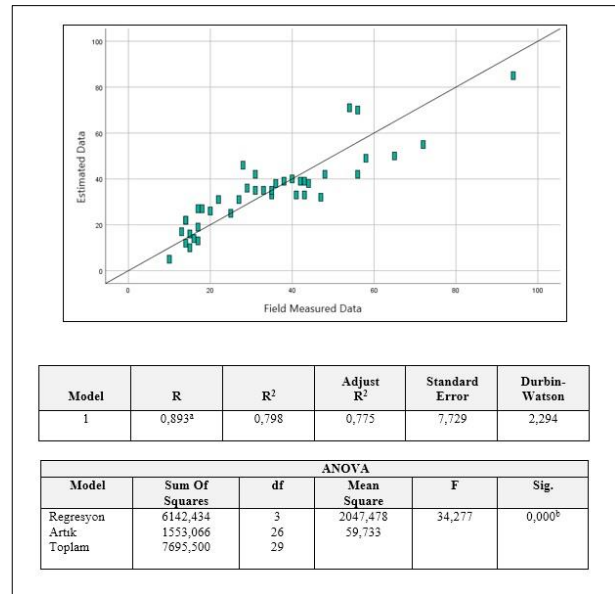


Figure 7. First regression analysis model

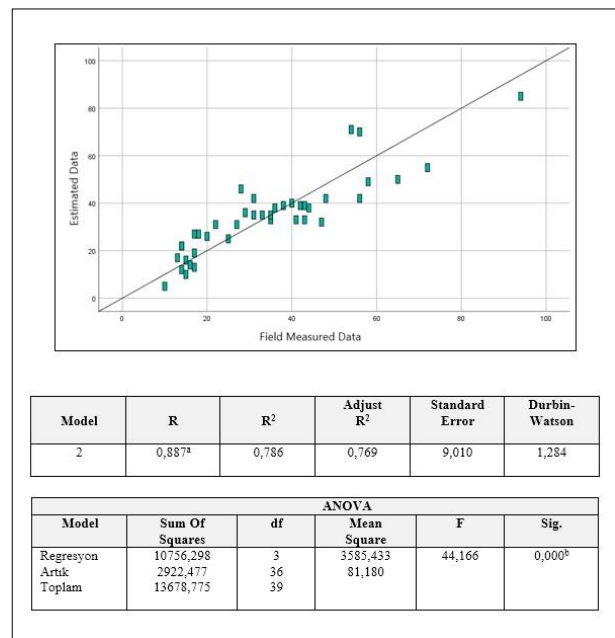


Figure 8. Second regression analysis model

3.3 Production of thematic maps

A model flowchart has been created for the generation of PM₁₀-related satellite images using coefficients derived from regression analysis. Both satellite images use the same model flow, but only the coefficients of the red, green and blue bands obtained by regression analysis

vary. The first input data of the installed model is the Sentinel-2 satellite image, which is truncated by its workspace. Regression coefficients were multiplied by red, green, and blue bands, and the resulting output data were collected to produce the associated satellite image of PM₁₀. These images were then classified, resulting in thematic maps of both terrain periods (Figure 9 and Figure 10).

In this study, two field studies were conducted in April and November. PM₁₀ maps were produced using satellite images closest to these dates. The main reason for this date difference between the studies is to accurately determine the impact of fossil fuel use and seasonal conditions on the study. The results obtained for two different dates enable a more meaningful interpretation of air pollution in the city center and the evaluation of other factors that cause pollution.

In the thematic map associated with PM₁₀, produced from a satellite image of 22.11.2021, the density of the city center ranges from 20 to 50 µg/m³ and 50 to 100 µg/m³, while traffic flow varies from 40 to 70 µg/m³ on intercity roads with heavy traffic, and 40 to 70 µg/m³ and 70 to 150 µg/m³ in the small industrial site and nearby region.

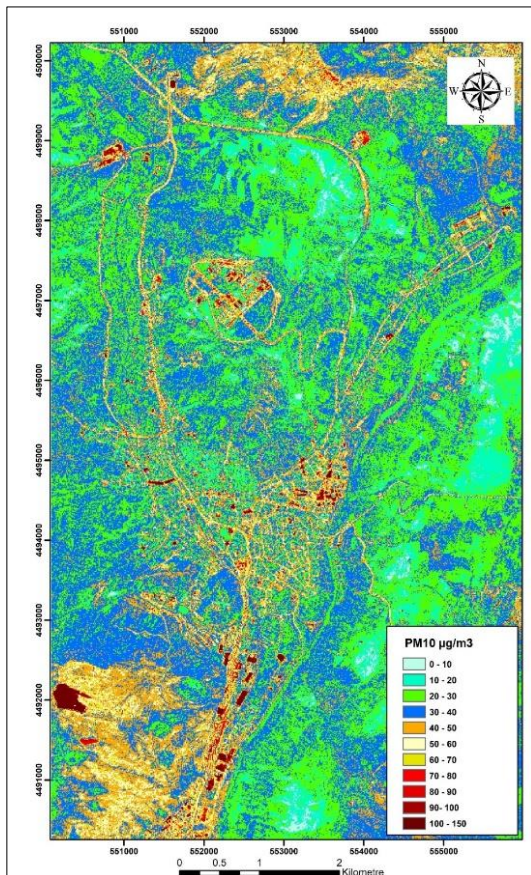


Figure 9. PM₁₀ thematic map dated 22.11.2021

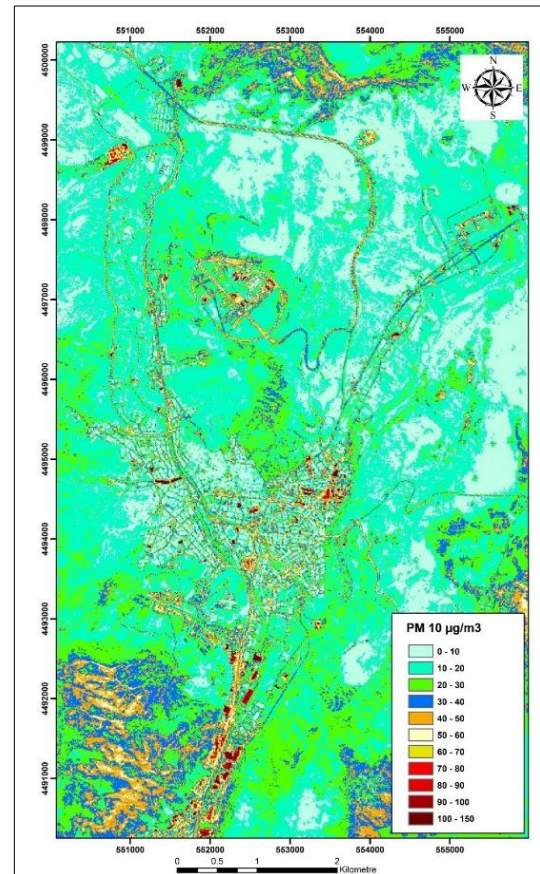


Figure 10. PM₁₀ thematic map dated 16.04.2022

In the thematic map associated with PM₁₀, produced from a satellite image of 16.04.2022, the density of the city center in the PM₁₀ range ranges from 0 to 30 µg/m³, while traffic flow between 30 and 70 µg/m³ on intercity roads where it is dense, and between 30 and 70 µg/m³ and 70 to 150 µg/m³ in the small industrial site and nearby.

The PM₁₀ values were outpaced by the index value of the air quality specified by the WHO in certain areas of the city center, the intercity roads and the small industrial site and its immediate area. High levels of PM₁₀ in the city center are thought to be caused by fossil fuel usage and vehicle emissions. The small industrial site and the high levels in its immediate vicinity originate from industrial facilities that operate within the region. The city-wide road is expected to be removed from the center of the city and the intercity connection to be established via an alternative freeway, resulting in better air quality in their habitats. It is also predicted that by moving industrial facilities away from the city center, the air quality of their living space can be improved, and industrial plant-generated air pollution can be reduced.

The determination coefficient values describing the extent of the relationship between PM₁₀ and Sentinel-2 satellite images were found in satellite image 0.893 on

22.11.2021 and 0.887 on 16.04.2022. These values indicate that the PM₁₀ parameters can be estimated using satellite images, such as in the work of Othman et al. (2010), Wang et al. (2021), Mamić et al. (2023), Nguyen and Tran (2014), and Chen et al. (2021). In addition, the failure of the fieldwork to perform the Sentinel-2 satellite images on the same day as the acquisition dates results in a relatively low deterministic coefficient. With the addition of PM₁₀ instances simultaneously from more dots and satellite images, or by choosing the passive sampling method instead of the portable sampling method used, the work accuracy can be improved.

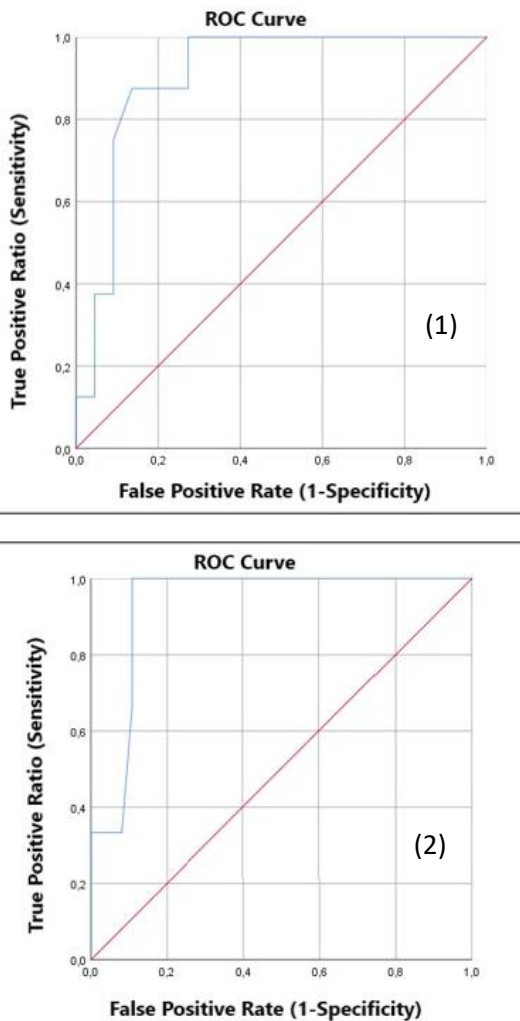


Figure 11. ROC curves generated by analysis

3.4 Statistical accuracy analysis

An ROC curve is a curve with true positive (sensitivity) rates on the vertical axis and false positive (1-specificity) rates on the horizontal axis for different threshold values. Each point on the ROC curve reveals the sensitivity and 1-specificity values corresponding to different threshold values (Tomak and Bek 2010). The ROC curve is formed by combining the intersection points of the sensitivity and

(1-specificity) points on the coordinate axis (Krzanowski and Hand 2009). ROC curves were drawn to analyze the accuracy of the thematic maps obtained in the study. Thematic maps produced for both terrain periods were compared to the test data which was randomly selected at about 20% before the model, with the value PM₁₀ given, and the ROC (Receiver Operating Characteristic) curves were drawn in this scope. Analysis shows that the area under the ROC curve shows thematic map accuracy of 90.6% for the first fieldwork and 93.2% for the second terrain study (Figure 11).

4. Conclusion

In this study, PM₁₀ parameters causing air pollution in Çankırı city center were estimated using Sentinel-2 satellite images. Two field studies were conducted to measure PM₁₀ parameters. The relationship between the red, green and blue bands of the Sentinel-2 satellite and the PM₁₀ data measured in field works was established by multiple regression analysis. Regression analyses yielded correlation coefficients of 0.80 and 0.79, respectively. A model was developed using the coefficients obtained from the regression analysis and the reflectance values of the Sentinel-2 satellite image. The PM₁₀ related satellite images obtained as a result of the model were classified, and thematic maps were produced.

The results of the study show that there are significant relationships between the reflectance values of the bands of Sentinel-2 satellite imagery and in-situ measured PM₁₀ parameters. Therefore, it is concluded that Sentinel-2 satellite imagery can be used to estimate PM₁₀ parameters that cause air pollution.

Declaration of Ethical Standards

The authors declare that they comply with all ethical standards.

Credit Authorship Contribution Statement

Author-1: Conceptualization, investigation, methodology and software, visualization and writing – original draft, review and editing.

Author-2: Conceptualization, methodology, supervision, review.

Declaration of Competing Interest

The authors declare that they have no known competing financial interests or personal relationships that could have appeared to influence the work reported in this paper.

Data Availability Statement

All data generated or analyzed during this study are included in this published article.

Acknowledgement

We would like to thank the T.C Ministry of Environment, Urbanization and Climate Change for their support in providing the data needed for this study.

5. References

- Anderson, J.O., Thundiyil, J.G., Stolbach, A., 2012. Clearing the air: a review of the effects of particulate matter air pollution on human health. *Journal of medical toxicology: official journal of the American College of Medical Toxicology*, **8(2)**, 166–175.
<https://doi.org/10.1007/s13181-011-0203-1>
- Chen, C.W., Tseng, Y.S., Mukundan, A., Wang, H.C., 2021. Air pollution: Sensitive Detection of PM_{2.5} and PM₁₀ Concentration Using Hyperspectral Imaging, *Applied Sciences*, **11**.
<https://doi.org/10.3390/app11104543>
- Cohen, A.J., Anderson, H.R., Ostro, B., Pandey, K.D., Krzyzanowski, M., Kunzli N., Gutschmidt, K., Pope, A., Romieu, I., Samet, J.M., Smith, K., 2005. Comparative Quantification of Health Risks, Global and Regional Burden of Disease Attributable to Selected Major Risk Factors, Urban Air pollution, *Journal of Toxicology and Environmental Health*, 433–1354.
- De Donno, A., De Giorgi, M., Bagordo, F., Grassi, T., Idolo, A., Serio, F., Ceretti, E., Feretti, D., Villarini, M., Moretti, M., Carducci, A., Verani, M., Bonetta, S., Pignata, C., Bonizzoni, S., Bonetti, A., Gelatti, U., MAPEC_LIFE Study Group., 2018. Health Risk Associated with Exposure to PM₁₀ and Benzene in Three Italian Towns. *International journal of environmental research and public health*, **15(8)**, 1672.
<https://doi.org/10.3390/ijerph15081672>
- Ghasempour, F., Alihsan Şekertekin, A., Kutoğlu, Ş.H., 2021. Google Earth Engine based spatio-temporal analysis of air pollutants before and during the first wave COVID-19 outbreak over Turkey via remote sensing, *Journal of Cleaner Production*, **319**.
<https://doi.org/10.1016/j.jclepro.2021.128599>
- Harbula, J., 2010. Dependence of PM₁₀ Particles Concentration on Aerosol Optical Thickness Value from the MODIS Data.
- Hime, N., Marks, G., Cowie, C., 2018. A Comparison of the Health Effects of Ambient Particulate Matter Air Pollution from Five Emission Sources. *International Journal of Environmental Research and Public Health*, **15**, 1206.
<https://doi.org/10.3390/ijerph15061206>
- İnal, C., Turgut, B., Yiğit, C.Ö., 2002. Lokal Alanlarda Jeoit Ondülasyonlarının Belirlenmesinde Kullanılan Enterpolasyon Yöntemlerinin Karşılaştırılması (Comparison of Interpolation Methods Usset to Determine Geoid Corrugations in Local Areas), Selçuk Üniversitesi Jeodezi ve Fotogrametri Mühendisliği Öğretiminde 30. Yıl Sempozyumu, 16–18.
- Jafarian, H., Behzadi, S., 2020. Evaluation of PM_{2.5} Emissions in Tehran by Means of Remote Sensing and Regression Models, *Pollution*, **6**, 521–529.
- Karakoç, O., 2022. Uzaktan Algılama ve Coğrafi Bilgi Sistemleri Entegrasyonu ile Çankırı İli Hava Kalitesi Haritasının Oluşturulması (Mapping of Dispersion of Air Quality of Çankırı Province by the Integration of Remote Sensing and Geographical Information Systems), (Master Thesis), Instute of Science, Konya, 96.
- Kim K. H., Kabir, E., Kabir, S., 2015. A Review on the Human Health Impact of Airborne Particulate Matter, *Environment International*, **74**, 136–143.
<https://doi.org/10.1016/j.envint.2014.10.005>
- Krzanowski, W. J., Hand, D. J., 2009. ROC Curve for Continuous Data, Chapman and Hall/CRC.
<https://doi.org/10.1201/9781439800225>
- Li, Z., Roy, D. P., Zhang, H. K., Vermote, E. F., Huang, H., 2019. Evaluation of Landsat-8 and Sentinel-2A Aerosol Optical Depth Retrievals Across Chinese Cities and Implications for Medium Spatial Resolution Urban Aerosol Monitoring, *Remote Sensing*, **11**.
<https://doi.org/10.3390/rs11020122>
- Maddala, G. S., 2001. Introduction to Econometrics, John Wiley&Sons, New York.
- Makineci, H., Arikan, D., Alkan, D., Karasaka, L., 2023. Spatio-temporal Analysis of Sentinel-5P Data of Konya City Between 2019- 2021, **170**, 23-40.
- Mamić, L., Gašparović, M., Kaplan, G., 2023. Developing PM_{2.5} and PM₁₀ prediction models on a national and regional scale using open-source remote sensing data, *Environ Monit Assess* **195**, 644.
<https://doi.org/10.1007/s10661-023-11212-x>
- Mather, P. M., Koch, M., 2011. Computer Processing of Remotely-Sensed Images: An Introduction, 4th ed., *Wiley-Blackwell*, Chichester.
- Nas, B., Karabork, H., Berktaş, A., Ekercin, S., 2007. Assessing Water Quality in the Beyşehir Lake (Turkey) by the Application of GIS, Geostatistics and Remote Sensing.
- Nguyen, N. H. and Tran, V.A., 2014. Estimation of PM₁₀ from Aot of Satellite Landsat 8 Image over Hanoi City,

in: International Symposium on Geoinformatics for Spatial Infrastructure Development in Earth and Allied Sciences.

Othman, N., Mat Jafri, M. Z., San, L. H., 2010. Estimating Particulate Matter Concentration over Arid Region Using Satellite Remote Sensing: A Case Study in Makkah, Saudi Arabia, *Modern Applied Science*, **4**.
<https://doi.org/10.5539/mas.v4n11p131>

Schwarze, P. E., Ovrevik, J., Låg, M., Refsnes, M., Nafstad, P., Hetland, R. B., & Dybing, E, 2006. Particulate matter properties and health effects: consistency of epidemiological and toxicological studies. *Human & experimental toxicology*, **25(10)**, 559–579.
<https://doi.org/10.1177/096032706072520>

Sifakis, N., 1992. Mapping of Air Pollution Using SPOT Satellite Data, *Photogrammetric Engineering and Remote Sensing*, **58**, 1433-1437.

Sola, I., García-Martín, A., Sandonís-Pozo, L., Álvarez-Mozos, J., Pérez-Cabello, F., González-Audicana, M., Llovería, R. M., 2018. Assessment of atmospheric correction methods for Sentinel-2 images in Mediterranean landscapes, *International Journal of Applied Earth Observation and Geoinformation*, **73**, 63-76.
<https://doi.org/10.1016/j.jag.2018.05.020>.

Şahinler, S., 2000. En Küçük Kareler Yöntemi ile Doğrusal Regresyon Modeli Oluşturmanın Temel Prensipleri (Basic Principles of Linear Regression Modeling with Least Squares Method), *MKÜ Faculty of Agriculture Journal*, **5**, 57–73.

Tasic, M., Rajsic, S., Novakovic, V., Mijic, Z., 2006. Atmospheric Aerosols and Their Influence on Air Quality in Urban Areas, *Facta universitatis-series: Physics, Chemistry and Technology*, **4**, 83–91.
<https://doi.org/10.2298/FUPCT0601083T>

Tomak, L., Bek, Y., 2010. Deneysel Araştırma (Experimental Research), **27**, 58-65.

Valavanidis, A., Fiotakis, K., Vlachogianni, T., 2008. Airborne particulate matter and human health: toxicological assessment and importance of size and composition of particles for oxidative damage and carcinogenic mechanisms. *Journal of Environmental Science and Health, Part C*, **26(4)**, 339-362.
<https://doi.org/10.1080/10590500802494538>

Wang, Y., Yuan, Q., Li, T., Tan, S., Zhang, L., 2021. Full-coverage spatiotemporal mapping of ambient PM2.5

and PM10 over China from Sentinel-5P and assimilated datasets: Considering the precursors and chemical compositions, *Science of The Total Environment*, **793**.

<https://doi.org/10.1016/j.scitotenv.2021.148535>.

Internet sources

- 1- https://www.un.org/development/desa/pd/sites/www.un.org.development.desa.pd/files/wpp2022_summary_of_results.pdf
- 2- <https://www.who.int/news/item/04-04-2022-billions-of-people-still-breathe-unhealthy-air-new-who-data>